General Synthetic Details. All manipulations were carried out under dry, oxygen-free argon using standard Schlenk line and glove box techniques. Toluene and hexane were dried by refluxing over potassium for at least 3 days prior to distillation. The solvent was then transferred onto 4 Å molecular sieves and degassed with three freeze-pump-thaw cycles. Anhydrous rare-earth chlorides (Strem Chemicals) and ^{n}BuLi (1.6 M in hexanes, Acros Organics) were used as received. $NaCp^{Me}$, $(Cp^{Me})_3Y$, $(Cp^{Me})_3Dy$ and IMes were prepared according to literature procedures.[1,2] Elemental analyses were carried out at London Metropolitan University, UK. IR spectra were recorded using solid samples on a Bruker Alpha Diamond ATR spectrometer. NMR spectra were recorded on a Bruker Avance-III 400 MHz spectrometer. X-Ray diffraction data was obtained from an Oxford Instruments XCalibur2 diffractometer, an Agilent SuperNova using MoKα radiation or a Bruker Prospector APEX-II using CuKα radiation. Structures were solved in Olex2 with SHELXT using intrinsic phasing and refined with SHELXL using least squares minimisation.[4-6] Analysis of the data for $\mathbf{3_Y}$ and $\mathbf{3_{Dy}}$ using the TWINROTMAT routine in PLATON[3] indicated the presence of minor twin components. In both cases the data were refined as 2 competent twins with BASF = 0.275(3) and 0.149(2) for $\mathbf{3_Y}$ and $\mathbf{3_{Dy}}$ respectively.

$[(Cp^{Me})_2Y(^{n}Bu)]_2$ ($\mathbf{1_Y}$). ^{n}BuLi (5.74 mL, 1.6 M in hexanes) was added to a suspension of $(Cp^{Me})_3Y$ (3.00 g, 9.2 mmol) in hexane (150 mL) at –78°C. Once the addition was complete, the resulting thicker, pale-yellow suspension was allowed to warm to room temperature. On warming, the reaction mixture became clearer, then quickly lost its colour and a white precipitate formed. The white suspension was stirred at room temperature for 2 hours. The mixture was allowed to settle, filtered and the hexane removed *in vacuo*. The resulting white powder was washed with cold pentane (15 mL), dried under vacuum and isolated (2.00 g, 72%). Crystals suitable for X-ray diffraction were grown from a concentrated toluene solution stored at –30°C. **Elemental analysis**, found/% (calculated/%); C, 62.86 (63.16); H, 7.63 (7.62). **^{1}H NMR** (C_6D_6, 298.15 K, δ/ppm): 5.96 (t, $^3J_{HH}$ = 2.69 Hz, 8 H, Cp C*H*); 5.87 (t, $^3J_{HH}$ = 2.69 Hz, 8H, Cp C*H*); 2.09 (s, 12 H, Cp CH_3); 1.33 (sex, $^3J_{HH}$ = 7.18 Hz, 4H, γ-CH_2); 0.94 (t, $^3J_{HH}$ = 7.34 Hz, 6H, δ-CH_3); 0.44 (quin, $^3J_{HH}$ = 8.56 Hz, 4H, β-CH_2); -0.44 (tt, $^3J_{HH}$ = 8.56 Hz, $^2J_{YH}$ = 1.47 Hz 4H, α-CH_2). **^{13}C NMR** (C_6D_6, 298.15 K, δ/ppm): 120.4 (Cp*C*-$(CH)_2$); 112.87 (Cp*C*H); 109.62 (Cp*C*H); 38.58 (α-*C*H_2); 32.53 (β-*C*H_2); 30.68 (γ-*C*H_2); 15.75 (*Me*Cp); 14.16 (δ-*C*H_3). **IR** (solid) ν_{max} (cm^{-1}): 2950 (w), 2923 (w), 2866 (w), 1454 (w), 1376 (w), 1046 (w), 1031 (m), 969 (w), 945 (w), 931 (w), 824 (m), 752 (s), 621 (m), 492 (m).

$[(Cp^{Me})_2Dy(^{n}Bu)]_2$ ($\mathbf{1_{Dy}}$). Compound $\mathbf{1_{Dy}}$ was synthesised in an identical manner to $\mathbf{1_Y}$ using $(Cp^{Me})_3Dy$ (3.00 g, 7.5 mmol) and ^{n}BuLi (4.7 mL, 1.6 M in hexanes). Yield (2.21 g, 78 %). Crystals suitable for X-ray diffraction were grown from a concentrated toluene solution stored at -30°C. **Elemental analysis**; found/% (calculated)/%; C, 50.67 (50.86); H, 6.02 (6.14). **IR** (solid) ν_{max} (cm^{-1}): 2950 (w), 2923 (w), 2866 (w), 1454 (w), 1046 (w), 1030 (m), 969 (w), 931 (w), 824 (m), 751 (s), 621 (m), 489 (m).

$[(Cp^{Me})_2Y(C_5H_4)FeCp]_2$ ($\mathbf{2_Y}$). Toluene (11 mL) was added to $\mathbf{1_Y}$ (0.669 g, 1.1 mmol) and ferrocene (0.409 g, 2.2 mmol) at room temperature with stirring. Once all the solids were dissolved the mixture was left to stand at room temperature. Large, dark red crystals formed after 24 hrs and more crystals continued to form over the next 3 days. The solution was decanted and the crystals dried under reduced pressure and isolated (0.474 g, 50%). **Elemental analysis**; found/% (calculated)/%; C, 61.19 (61.14); H, 5.37 (5.36). **^{1}H NMR** (d_8-THF, 298.15 K, δ/ppm): 6.04 (s, 16 H, Cp^{Me}C-*H*); 4.01 (t, $^3J_{HH}$ = 1.35 Hz, 4H, FeC_5H_4-C*H*); 3.97 (s, 10H, FeCp*H*); 3.96 (t, $^3J_{HH}$ = 1.74 Hz, 4H, FeC_5H_4-C*H*); 2.18 (s, 12H, *Me*Cp). **^{13}C NMR** (d_8-THF, 298.15 K, δ/ppm): 129.72 (Y-C_5H_4-Fe); 122.29 (Cp^{Me}*C*-$(CH)_2$); 111.78 (Cp^{Me}*C*H); 110.42 (Cp^{Me}*C*H); 99.9 (Fe-C_5H_4); 99.27 (Fe-C_5H_4); 79.77 (Fe-C_5H_4); 70.37 (Fe-C_5H_4); 67.25 (Fe-C_5H_5); 15.24 ($Cp^{Me}CH_3$). **IR** (solid) ν_{max} (cm^{-1}): 3083 (w), 2961 (w), 2922 (w), 2895 (w), 2859 (w), 1410 (w), 1107 (w), 1084 (w), 1075 (w), 1050 (w), 1032 (w), 1010 (m), 931 (w), 831 (m), 747 (s), 623 (w), 503 (m), 478 (w).

$[(Cp^{Me})_2Dy(C_5H_4)FeCp]_2$ ($\mathbf{2_{Dy}}$). Compound $\mathbf{2_{Dy}}$ was synthesised in a similar manner to $\mathbf{2_Y}$ using $\mathbf{1_{Dy}}$ (0.248 g, 0.33 mmol) and ferrocene (0.122 g, 0.657 mmol). Yield (0.18 g, 54 %). **Elemental analysis**; found/% (calculated)/%; C, 52.32 (52.24); H, 4.67 (4.58). **IR** (solid) ν_{max} (cm^{-1}): 3082 (w), 2961 (w), 2922 (w), 2895 (w), 2859 (w), 1455 (w), 1410 (w), 1380 (w), 1107 (w), 1084 (w), 1075 (w), 1049 (w), 1032 (w), 1010 (m), 931 (w), 831 (m), 747 (s), 622 (w), 503 (m), 478 (w).

$[(Cp^{Me})_2Y(IMes')]$ ($\mathbf{3_Y}$). A solution of IMes (0.100 g, 0.33 mmol) in toluene (3 mL) was added dropwise to a solution of $\mathbf{1_Y}$ (0.100 g, 0.16 mmol) in toluene (3 mL) at RT. Upon addition of IMes there was an immediate colour change from colourless to bright yellow. The mixture was left to stand at RT for 1.5 hrs then the

solution was evaporated to dryness, affording a yellow powder, which was recrystallized from a concentrated toluene solution stored at –30°C. (0.154 g, 85 %). **Elemental analysis**, found/% (calculated)/%; C, 71.8 (71.98); H, 6.86 (6.77); N, 4.85 (5.08). **^{1}H NMR** (C_6D_6, 298.15 K, δ/ppm): 6.95 (s, 1 H, ArC-H); 6.72 (s, 1 H, ArC-H); 6.70 (s, 1 H, ArC-*H*); 6.48 (d, $^3J_{HH}$ = 1.59 Hz, 1 H, C=C(N)-*H*); 6.38 (s, 1 H, ArC-*H*); 6.12 (d, $^3J_{HH}$ = 1.59 Hz, 1 H, C=C(N)-*H*); 5.94 (qr, $^3J_{HH}$ = 2.84 Hz, 1 H, CpC-*H*); 5.90 (m, 2 H, CpC-*H*); 5.63 (qr, 1 H, CpC-*H*); 5.60 (qr, 1 H, CpC-*H*); 5.55 (qr, 1 H, CpC-*H*); 5.40 (qr, $^3J_{HH}$ = 2.84 Hz, 1 H, CpC-*H*); 5.15 (qr, $^3J_{HH}$ = 2.84 Hz, 1 H, CpC-*H*); 2.28 (s, 3 H, Ar-CH_3); 2.16 (s, 3 H, Ar-CH_3); 2.10 (s, 3 H, Ar-CH_3); 2.07 (d, $^3J_{HH}$ = 2.84 Hz, 1 H, Y-C*H*); 2.05 (s, 3 H, Ar-CH_3); 2.04 (s, 3 H, Ar-CH_3); 1.95 (s, 3 H, Cp-CH_3); 1.93 (s, 3 H, Cp-CH_3); 1.12 (dd, $^2J_{HH}$ = 3.47 Hz, 1 H, Y-C*H*). **^{13}C NMR** (C_6D_6, 298.15 K, δ/ppm): 194.74 (N*C*N); 194.35 (C=*C*(N)-H); 184.46 (C=*C*(N)-H); 152.77 (Ar*C*-N); 139.3 (Ar*C*-N); 138.13 (Ar*C*-CH_2); 136.95 (Ar*C*-H); 135.05 (Ar*C*-H); 135.02 (Ar*C*-H); 130.31 (Ar*C*-H); 129.87 (Ar*C*-CH_3); 124.14 (Ar*C*-CH_3); 123.89 (Ar*C*-CH_3); 122.78 (Ar*C*-CH_3); 121.48 (Ar*C*-CH_3); 120.49 (Cp*C*-$(CH)_2$); 120.01 (Cp*C*-$(CH)_2$); 112.98 (Cp*C*H); 111.38 (Cp*C*H); 110.92 (Cp*C*H); 110.31 (Cp*C*H); 110.15 (Cp*C*H); 109.19 (Cp*C*H); 108.91 (Cp*C*H); 108.75 (Cp*C*H); 48.43 (Ar-*C*H_3); 48.3 (Ar-*C*H_3); 21.78 (Ar-*C*H_3); 21.21 (Ar-*C*H_3); 20.0 (Ar-*C*H_3); 18.79 (Y-*C*H_2); 15.58 (*Me*Cp); 15.05 (*Me*Cp). **IR** (solid) ν_{max} (cm^{-1}); 2957 (w), 2922 (w), 2896 (w), 2858 (w), 1586 (w), 1557 (w), 1487 (w), 1389 (w), 1266 (m), 1168 (w), 929 (w), 858 (m), 810 (s), 756 (s), 735 (s), 684 (w), 659 (w), 625 (w), 596 (w), 566 (m), 549 (w), 521 (w), 496 (w), 465 (w).

[$(Cp^{Me})_2$Dy(IMes')] ($\mathbf{3_{Dy}}$). Compound $\mathbf{3_{Dy}}$ was synthesised in an identical manner to $\mathbf{3_Y}$ using $\mathbf{1_{Dy}}$ (0.124 g, 0.16 mmol) and IMes (0.100 g, 0.33 mmol). Yield: (0.175 g, 86 %). Crystals suitable for X-ray diffraction were grown by slow evaporation of a toluene solution at RT. Elemental analysis; found/%; (calculated)/%: C, 63.38 (63.51); H, 6.05 (5.97); N, 4.48 (4.48). **IR** (solid) ν_{max} (cm^{-1}); 2962 (w), 2922 (w), 2895 (w), 2857 (w), 1587 (w), 1569 (w), 1488 (w), 1459 (w), 1445 (w), 1392 (w), 1380 (w), 1312 (w), 1298 (w), 1261 (m), 1241 (w), 1169 (w), 1096 (m), 1025 (s), 964 (w), 929 (w), 872 (m), 858 (m), 809 (s), 778 (s), 769 (s), 752 (s), 735 (s), 684 (w), 660 (w), 623 (w), 581 (w), 566 (m), 549 (w), 519 (w), 495 (w), 465 (w).

[$(Cp^{Me})_3$Y(*a*IMes)]·C_6H_6 ($\mathbf{4_Y}$). IMes (0.239 g, 0.79 mmol) was dissolved in benzene (3 mL) and added dropwise to a solution of $(Cp^{Me})_3$Y (0.256 g, 0.79 mmol) in benzene (3 mL) at RT. The reaction mixture was left to stand for five days during which time colourless crystals formed. The solution was decanted and the crystals washed with benzene to afford the product (0.453 g, 81 %). **Elemental analysis**; found/% (calculated)/%; C, 71.38 (76.2); H, 6.52 (7.25); N, 4.10 (3.95**^{1}H NMR** (C_6D_6, 298.15 K, δ/ppm): 6.78 (s, 2 H, ArC-*H*); 6.77 (d, $^3J_{HH}$ = 1.47 Hz, 1 H, N-C(*H*)-N); 6.64 (s, 2 H, ArC-*H*); 6.10 (d, $^3J_{HH}$ = 1.47 Hz, 1 H, N-C(*H*)-C-Y); 5.85 (t, 6 H, CpC-*H*); 5.60 (t, $^3J_{HH}$ = 1.59 Hz, 1 H, CpC-*H*); 2.37 (s, 9 H, Ar-CH_3); 2.11 (s, 3 H, Cp-CH_3); 2.10 (s, 3 H, Cp-CH_3); 1.81 (s, 6 H, Ar-CH_3). **IR** (solid) ν_{max} (cm^{-1}); 3052 (w), 2919 (w), 2857 (w), 1480 (w), 1457 (w), 1377 (w), 1226 (w), 1080 (w), 930 (w), 870 (w), 851 (w), 771 (s), 617 (w).

[$(Cp^{Me})_3$Dy(*a*IMes)]·C_6H_6 ($\mathbf{4_{Dy}}$). was synthesised in an identical manner to $\mathbf{4_{Dy}}$ using $(Cp^{Me})_3$Dy (0.100 g, 0.25 mmol) and IMes (0.076 g, 0.25 mmol). Yield: 0.132 g, 68 %. **Elemental analysis:** found/% (calculated)/%; C, 68.89 (69.08); H, 6.72 (6.57); N, 3.60 (3.58). **IR** (solid) ν_{max} (cm^{-1}); 3092 (w), 2919 (w), 2859 (w), 1545 (w), 1479 (w), 1376 (w), 1225 (w), 1080 (w), 1035 (w), 967 (m), 929 (w), 869 (w), 850 (w), 825 (m), 745 (s), 671 (s), 616 (w), 565 (w).

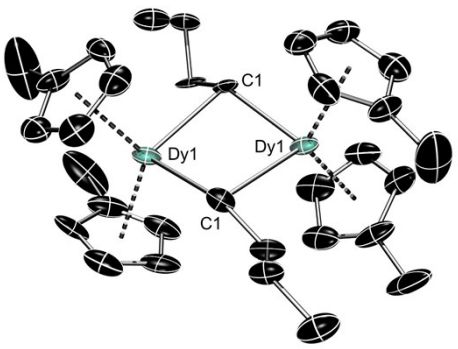

Figure S1. ORTEP representation of the molecular structure of $\mathbf{1_{Dy}}$. Thermal ellipsoids set at 50% probability. Hydrogen atoms are omitted for clarity. Selected bond lengths (Å) and angles (°): Dy(1)–C(1) 2.536(18), 2.591(18); Dy-Cp^{Me}_{cent} 2.382(13)-2.390(12); Cp^{Me}_{cent}-Dy-Cp^{Me}_{cent} 125.9(5).

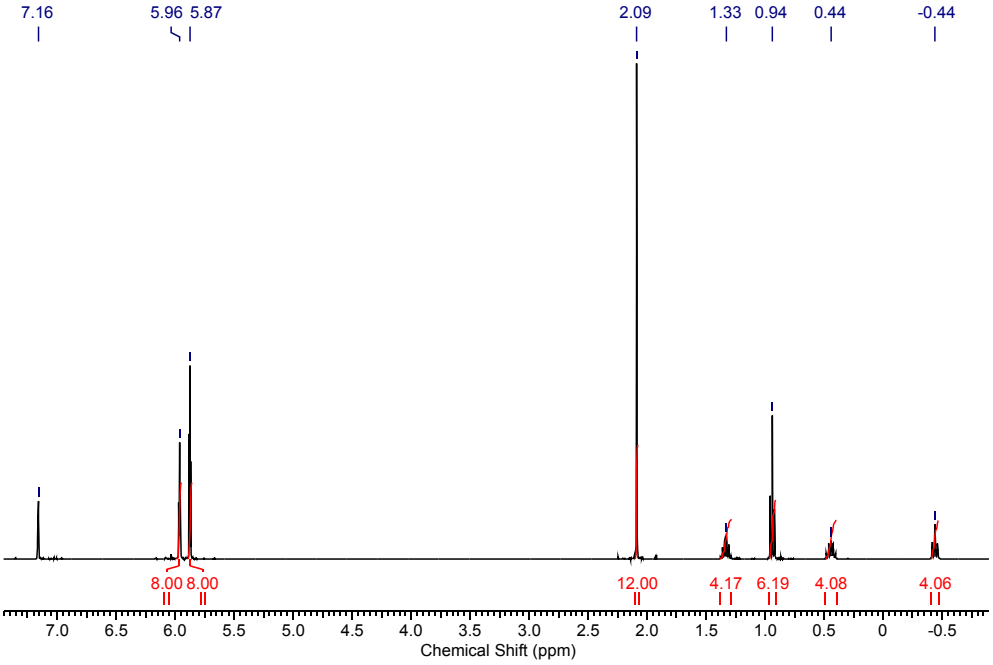

Figure S2. ^{1}H NMR spectrum of $\mathbf{1_Y}$ in benzene-d_6.

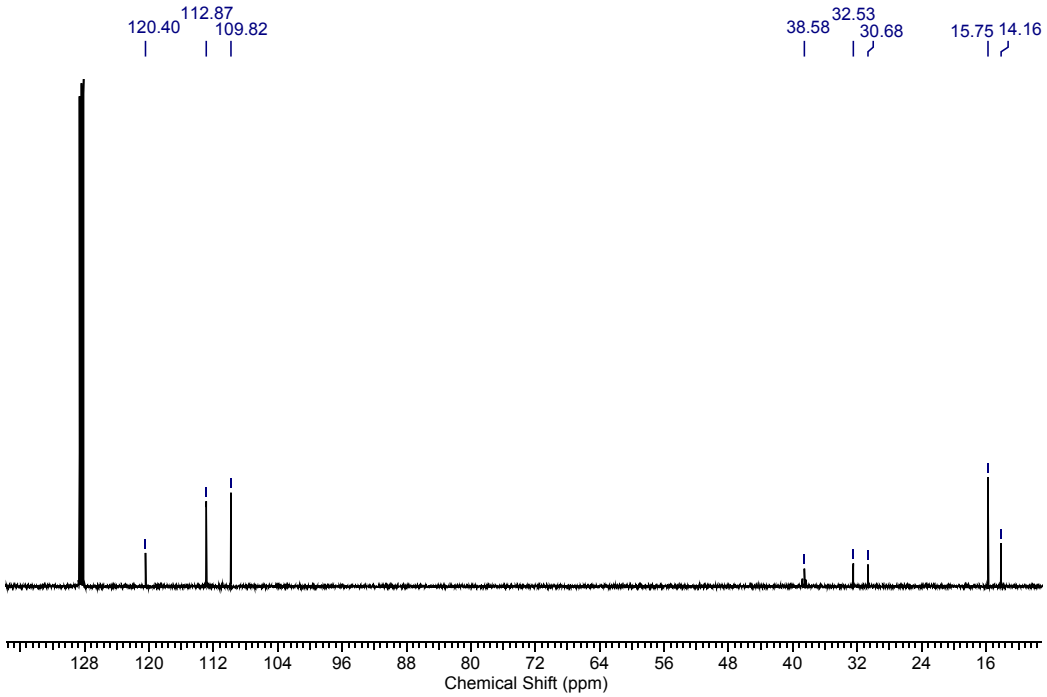

Figure S3. ^{13}C NMR spectrum of $\mathbf{1_Y}$ in benzene-d_6.

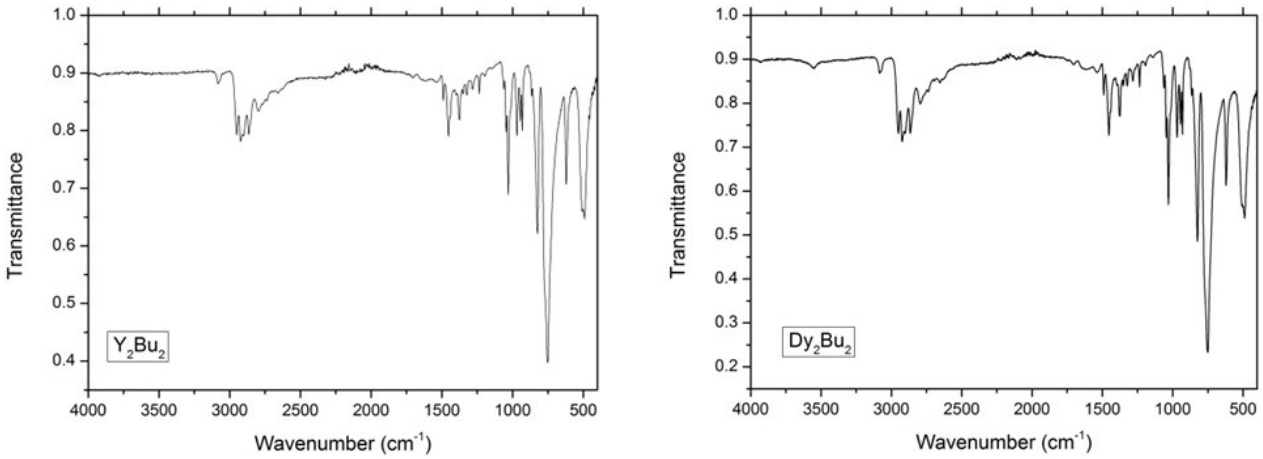

Figure S4. IR spectra of $\mathbf{1_Y}$ (left) and $\mathbf{1_{Dy}}$ (right).

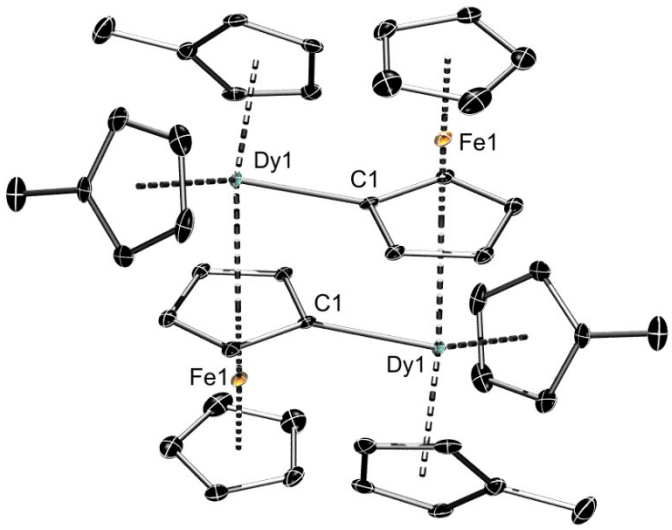

Figure S5. ORTEP representation of the molecular structure of $\mathbf{2_{Dy}}$. Thermal ellipsoids set at 50% probability. Hydrogen atoms are omitted for clarity. Selected bond lengths (Å) and angles (°): Dy(1)–C(1) 2.461(4) Å; Dy-Cp^{Me}_{cent} 2.421(2)-2.430(2) Å; Dy-$Cp(Fe)_{cent}$ 2.602(11) Å; Cp^{Me}_{cent}-Dy-Cp^{Me}_{cent} 121.43(7)°; C(1)-Dy(1)-$Cp(Fe)_{cent}$ 94.10(2)°.

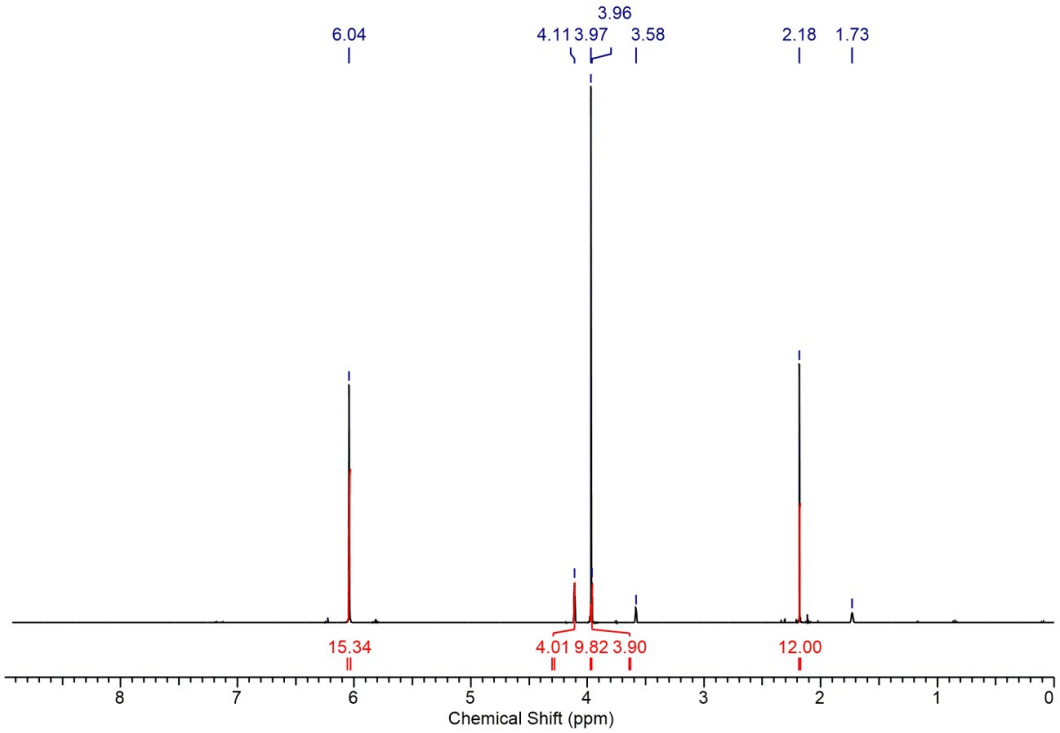

Figure S6. ^{1}H NMR spectrum of $\mathbf{2_Y}$ in THF-d_8.

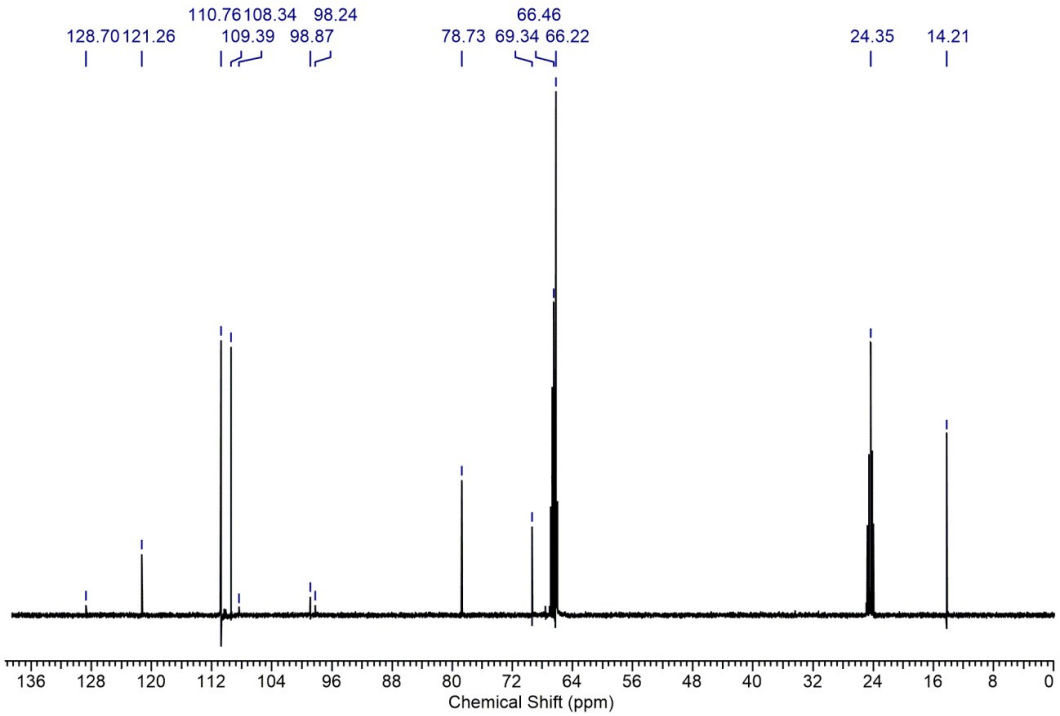

Figure S7. ^{13}C NMR spectrum of $\mathbf{2_Y}$ in THF-d_8.

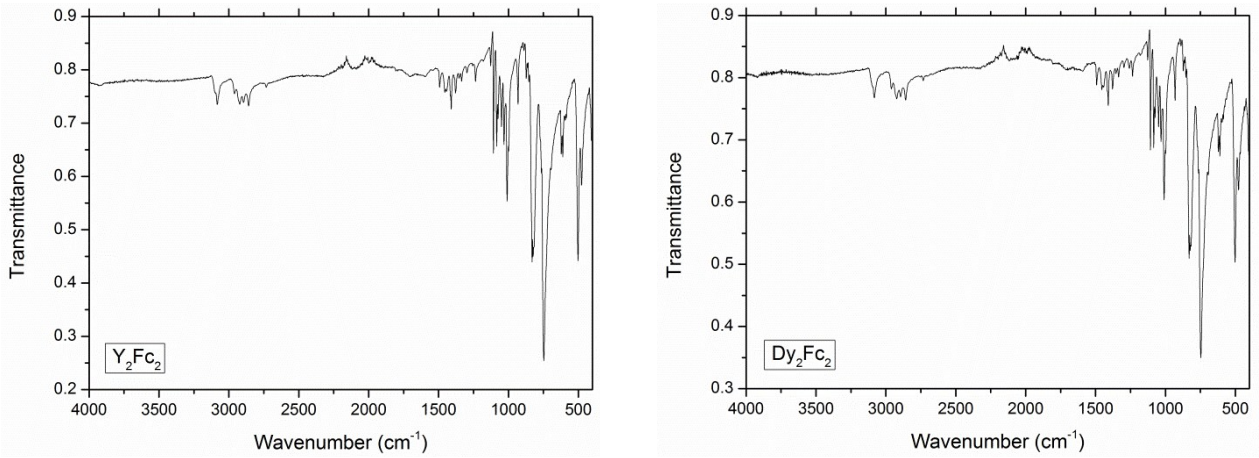

Figure S8. IR spectra of $\mathbf{2_Y}$ (left) and $\mathbf{2_{Dy}}$ (right).

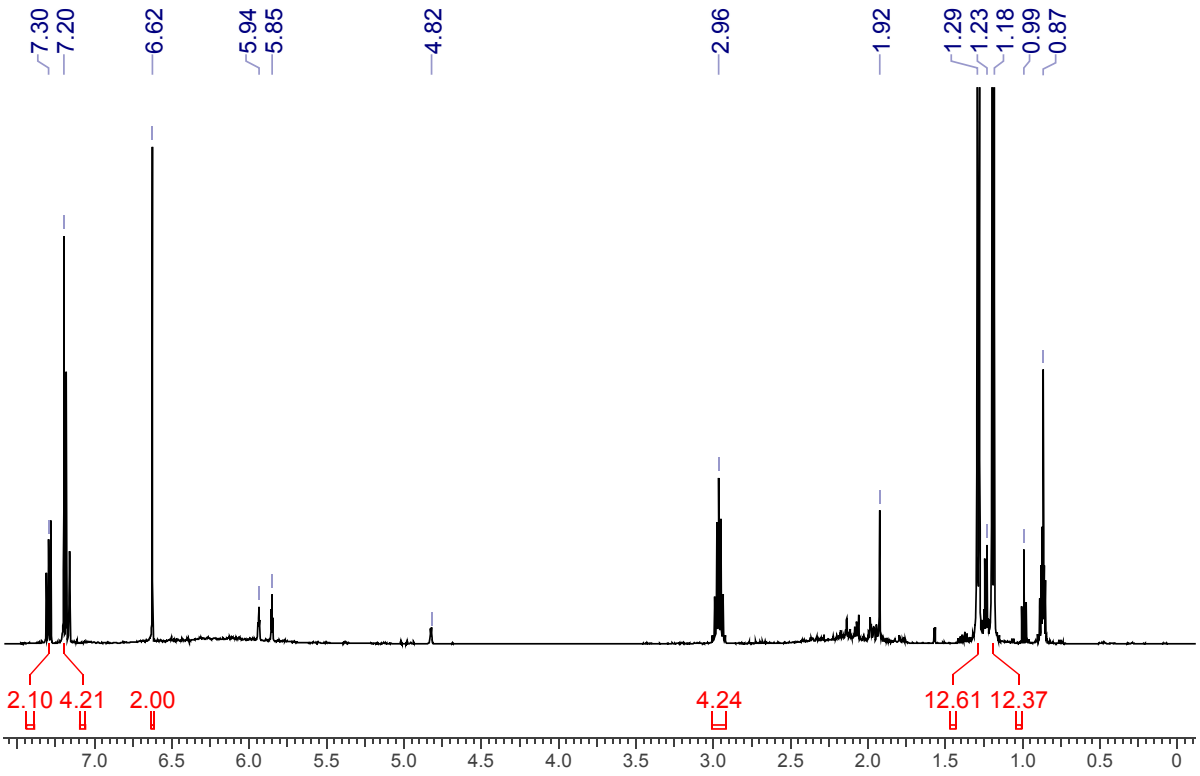

Figure S9. ^{1}H NMR spectrum of a mixture of $\mathbf{1_Y}$ and IPr in benzene-d_6 after stirring for two days at 293 K, followed by heating at 353 K for one day, assigned peaks correspond to IPr. ^{1}H NMR (C_6D_6, 500 MHz): δ 7.30 (t, 2H, J = 7.5 Hz, ArC*H*), 7.20 (d, 4H, J = 7.5 Hz, ArC*H*), 6.62 (s, 2H, N(*H*)C=C(*H*)N), 2.97 (sept, 4H, J = 6.9 Hz, H_3C-C(*H*)-CH_3), 1.29 (d, 12H, J = 6.9 Hz, H_3C-C(H)-CH_3) and 1.18 (d, 12H, J = 6.9 Hz, H_3C-C(H)-CH_3).

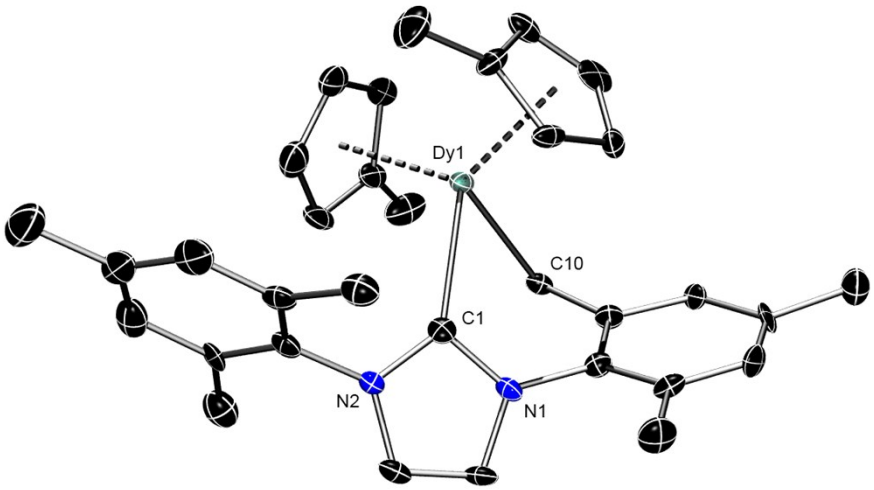

Figure S10. ORTEP representation of the molecular structure of $\mathbf{3_{Dy}}$. Thermal ellipsoids set at 50% probability. Hydrogen atoms are omitted for clarity. Selected bond lengths (Å) and angles (°): Dy(1)–C(1) 2.451(9) Å; Dy(1)–C(2) 2.534(9); Cp^{Me}_{cent}–Dy(1) 2.374(5)-2.375(6) Å; Cp^{Me}_{cent}-Dy(1)-Cp^{Me}_{cent} 128.55(15)°; C(2)-Dy(1)-C(1) 74.7(3)°.

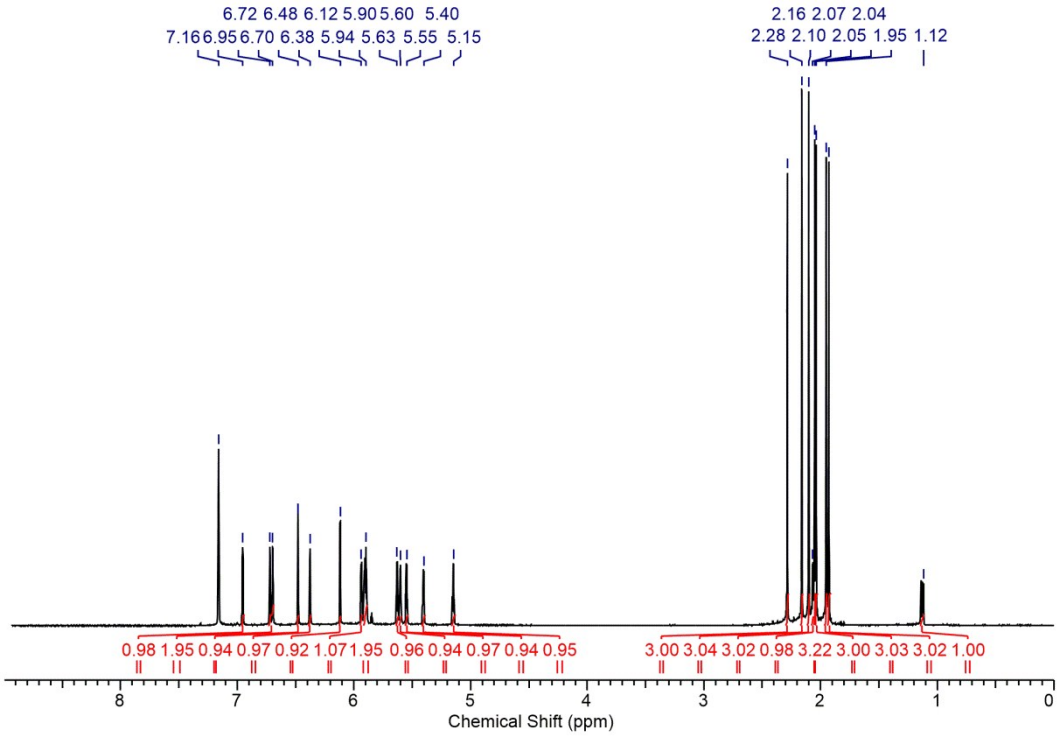

Figure S11. ^{1}H NMR spectrum of $\mathbf{3_Y}$ in benzene-d_6.

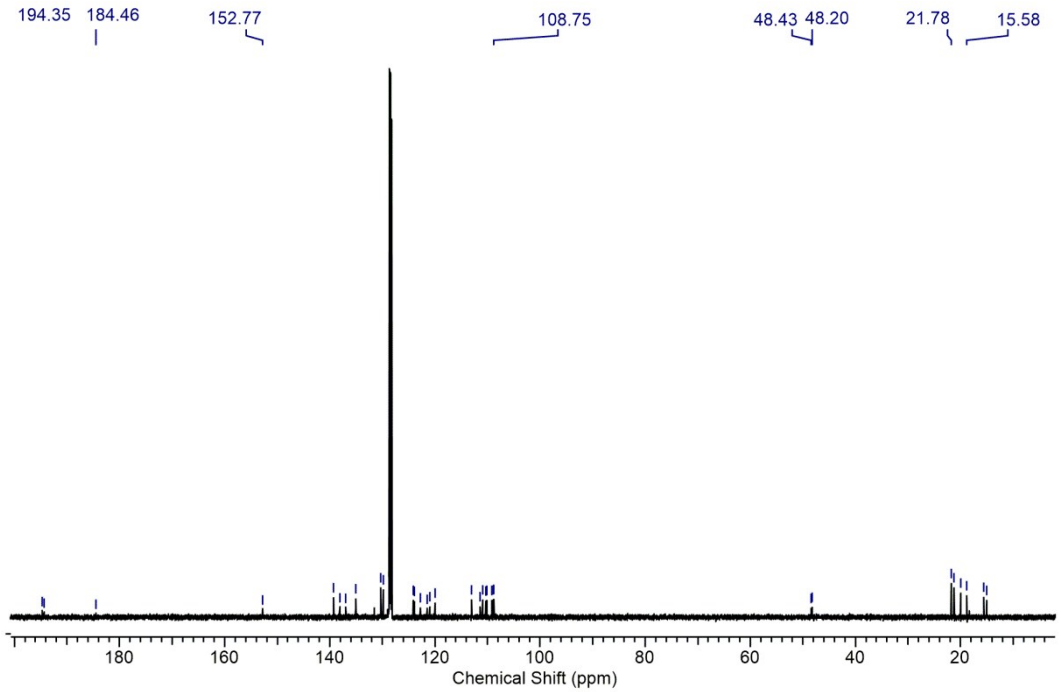

Figure S12. ^{13}C NMR spectrum of $\mathbf{3_Y}$ in benzene-d_6.

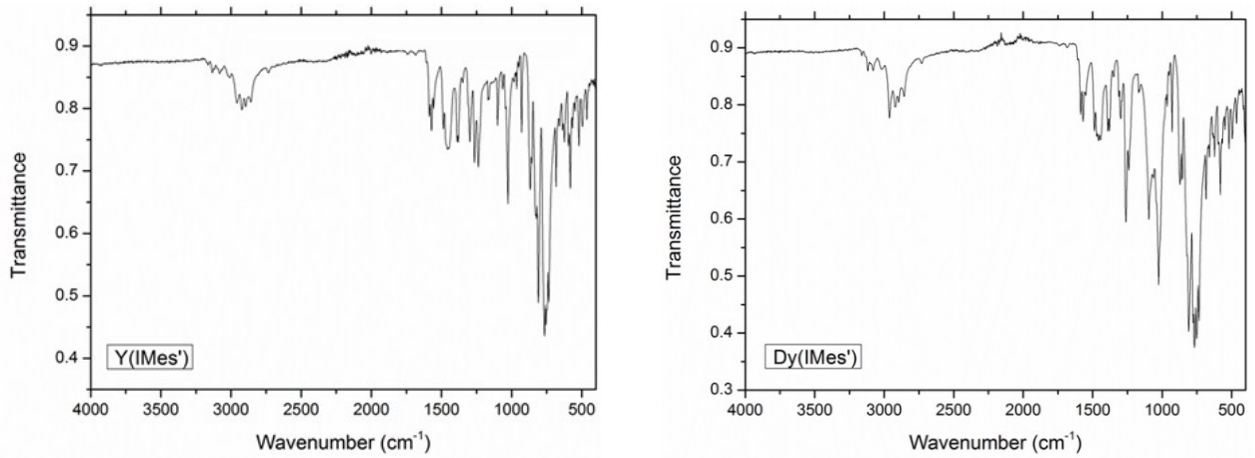

Figure S13. IR spectra of $\mathbf{3_Y}$ (left) and $\mathbf{3_{Dy}}$ (right).

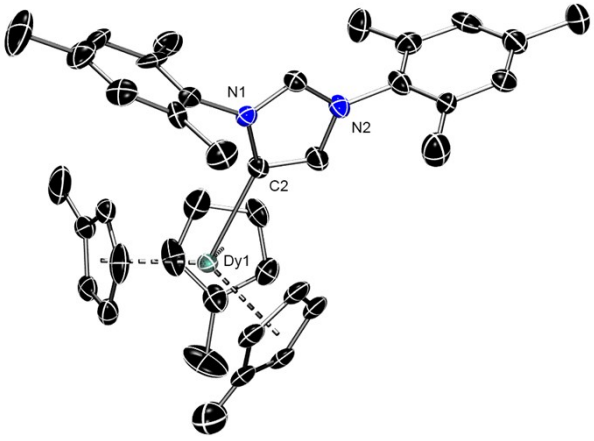

Figure S14. ORTEP representation of the molecular structure of $\mathbf{4_{Dy}}$. Thermal ellipsoids set at 50% probability. Hydrogen atoms are omitted for clarity. Selected bond lengths (Å) and angles (°): Dy(1)–C(1) 2.583(10) Å; Dy(1)–Cp^{Me}_{cent} 2.462(5)-2.526(5) Å; Cp^{Me}_{cent}-Dy(1)-C(1) 80.54(4)-106.4(4)°.

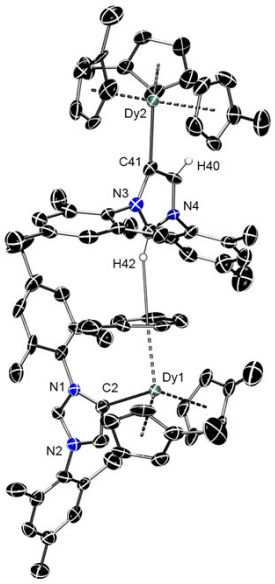

Figure S15. Extended molecular structure of $\mathbf{4_{Dy}}$ highlighting the short C–H···π interaction with an adjacent Cp^{Me} ring.

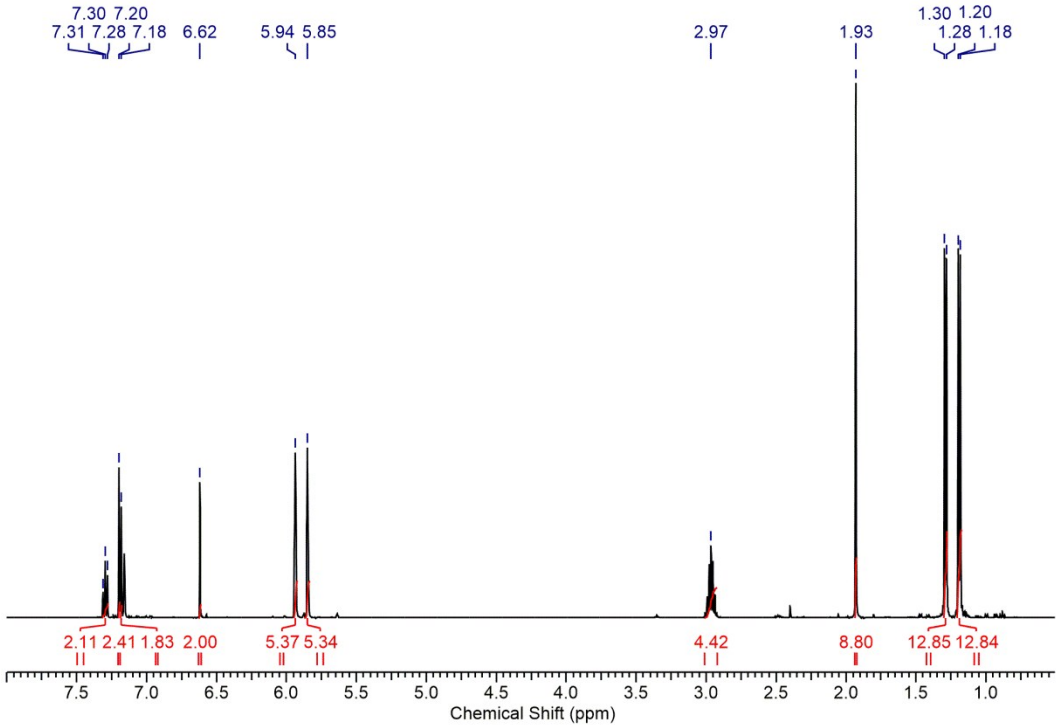

Figure S16. ^{1}H NMR spectrum of a mixture of Cp^{Me}_3Y and IPr in benzene-d_6 after stirring for two days at 293 K, followed by heating at 353 K for one day. ^{1}H NMR (C_6D_6, 500 MHz): δ 7.30 (t, 2H, J = 7.5 Hz, ArC*H*), 7.19 (d, 4H, J = 7.5 Hz, ArC*H*), 6.62 (s, 2H, N(*H*)C=C(*H*)N), 5.94 (t, 6H, J = 1.6 Hz, CpC-*H*), 5.85 (t, 6H, J = 1.6 Hz, CpC-*H*), 2.97 (sept, 4H, J = 6.9 Hz, H_3C-C(*H*)-CH_3), 1.93 (s, 9H, Cp-CH_3) 1.29 (d, 12H, J = 6.9 Hz, H_3C-C(H)-CH_3) and 1.19 (d, 12H, J = 6.9 Hz, H_3C-C(H)-CH_3).

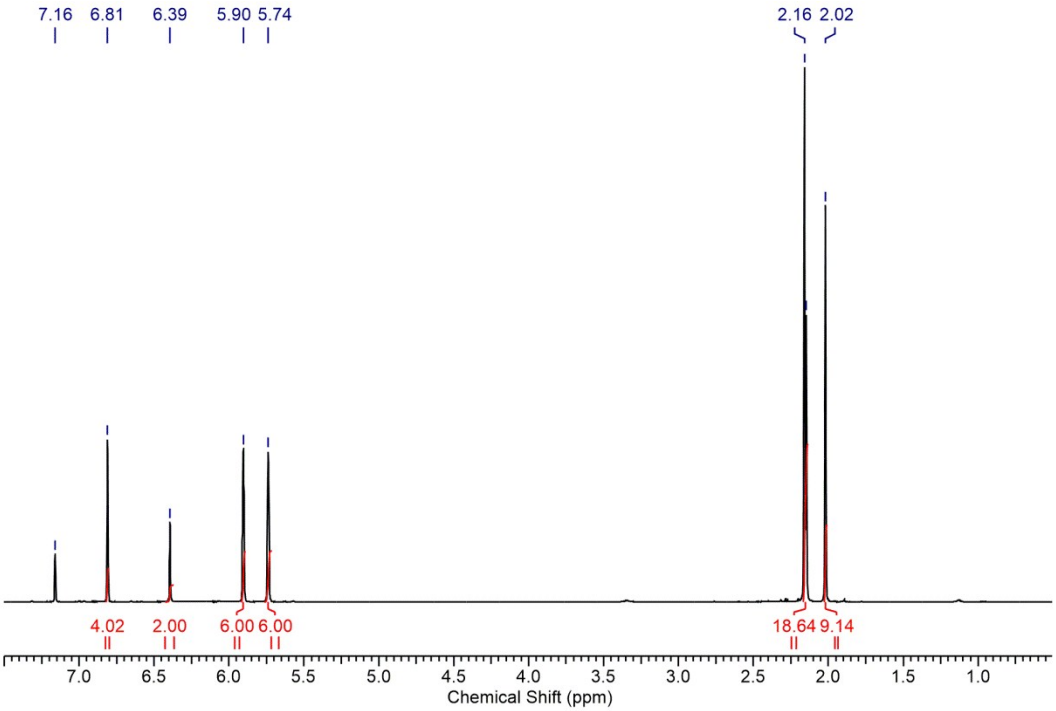

Figure S17. ^{1}H NMR spectrum of a mixture of $(Cp^{Me})_3Y$, IMes and $\mathbf{4_Y}$ in benzene-D_6, recorded 15 minutes after mixing.

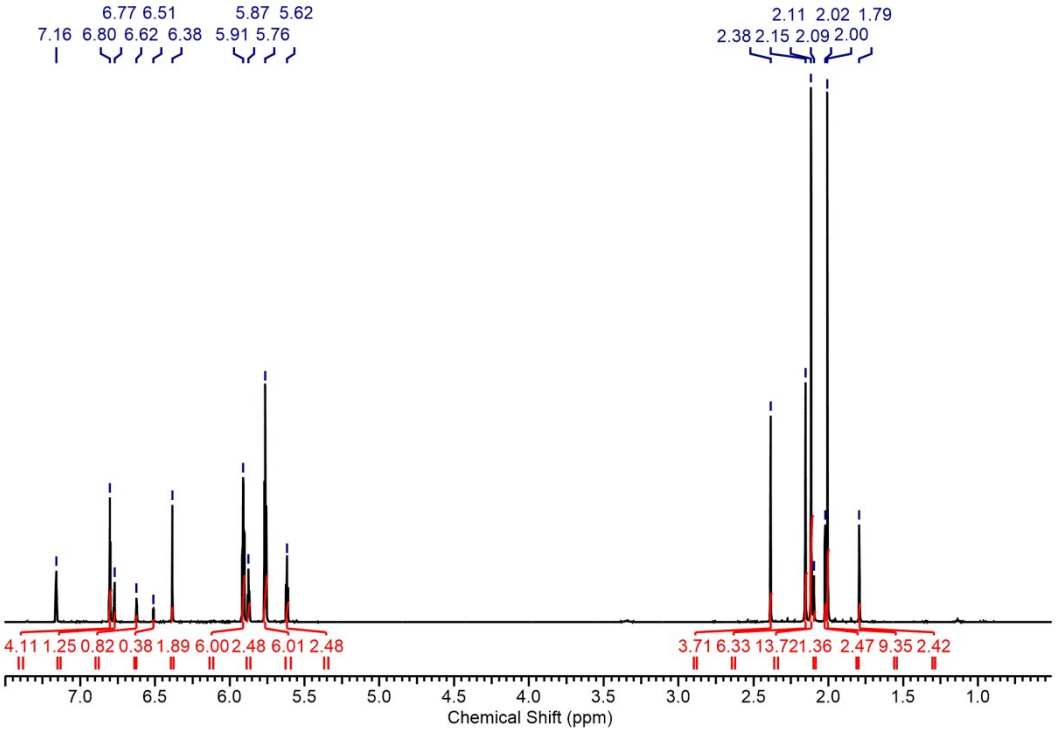

Figure S18. ^{1}H NMR spectrum of a mixture of $(Cp^{Me})_3Y$, IMes and $\mathbf{4_Y}$ in benzene-D_6, recorded 48 hours after mixing.

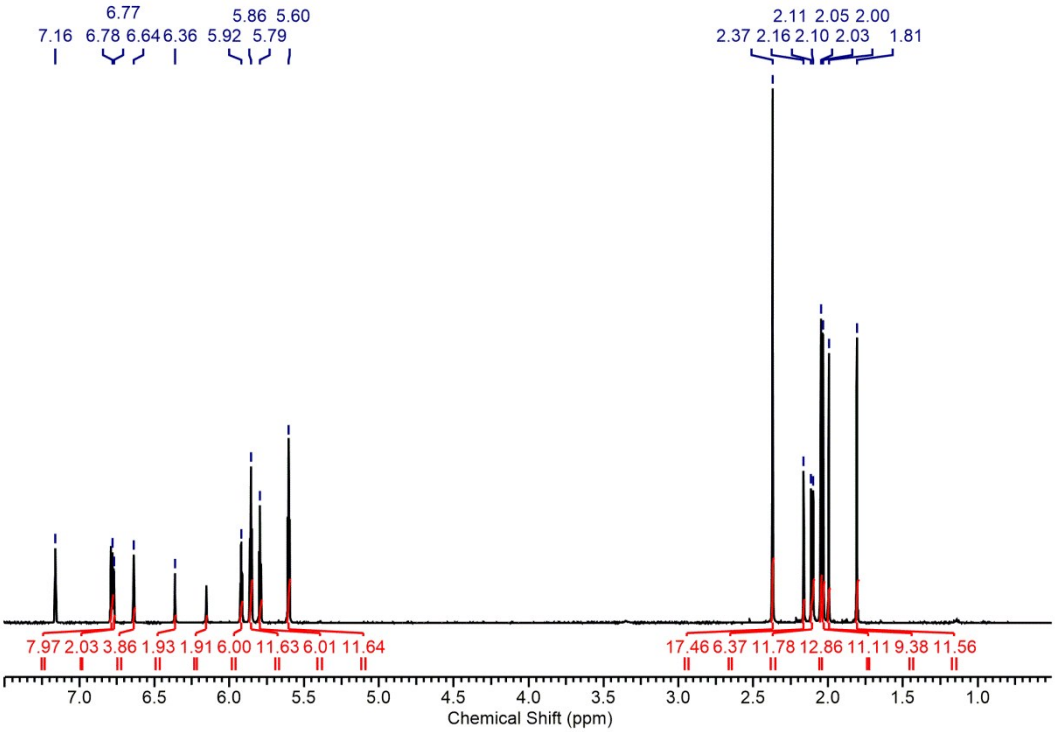

Figure S19. ^{1}H NMR spectrum of a mixture of $(Cp^{Me})_3Y$, IMes and $\mathbf{4_Y}$ in benzene-D_6, recorded 192 hours after mixing.

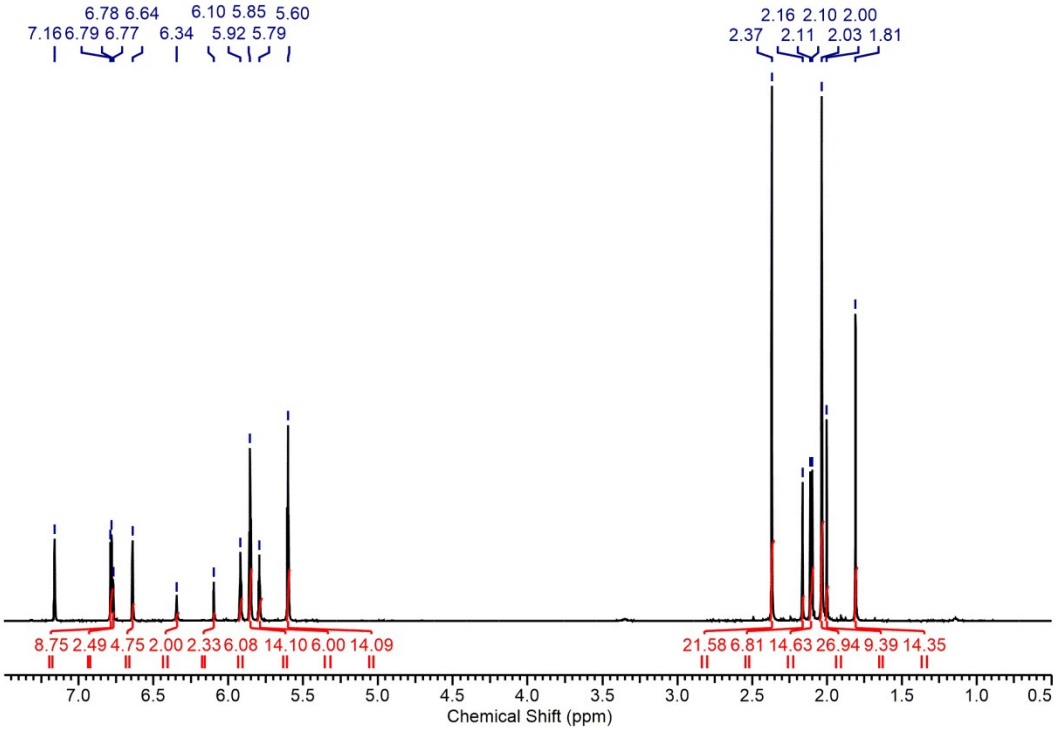

Figure S20. ^{1}H NMR spectrum of a mixture of $(Cp^{Me})_3Y$, IMes and $\mathbf{4_Y}$ in benzene-D_6, recorded 576 hours after mixing.

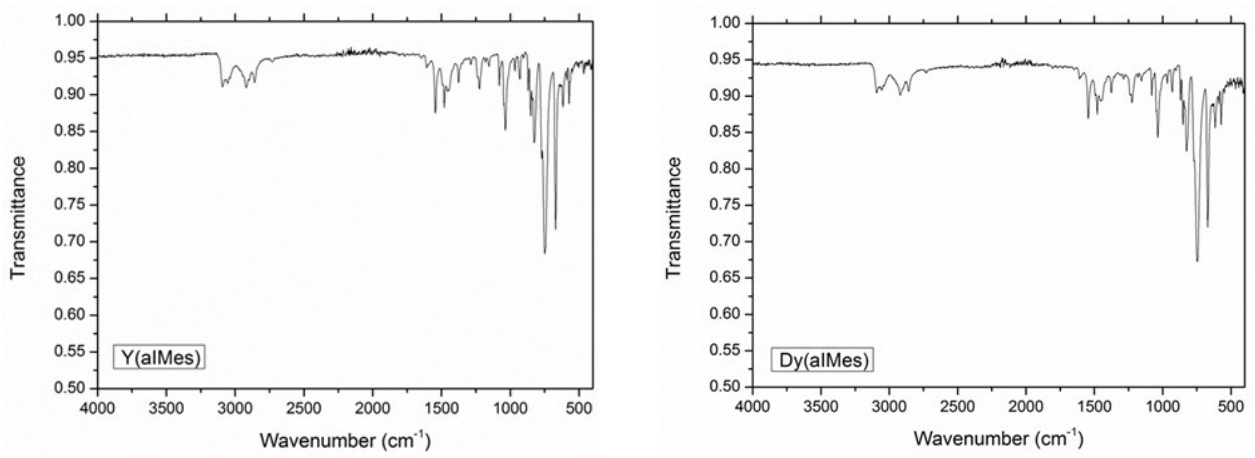

Figure S21. IR spectra of $\mathbf{4_Y}$ (left) and $\mathbf{4_{Dy}}$ (right).

Table S1. Crystal data and structure refinement details for $\mathbf{1_Y}$-$\mathbf{4_Y}$.

Compound	$\mathbf{1_Y}$	$\mathbf{2_Y}$	$\mathbf{3_Y}$	$\mathbf{4_Y}$
Empirical Formula	$C_{32}H_{46}Y_2$	$C_{44}H_{46}Fe_2Y_2$	$C_{33}H_{37}N_2Y$	$C_{90}H_{102}N_4Y_2$
Formula Weight	608.51	864.33	550.55	1417.57
Temperature/K	150.02(10)	150	150.01(12)	100.02(10)
Crystal System	Orthorhombic	Monoclinic	Monoclinic	Monoclinic
Space Group	$P2_12_12$	$P2_1/n$	$P2_1/c$	$P2_1/c$
a/Å	14.4805(4)	11.4603(11)	17.8886(16)	15.5723(8)
b/Å	15.4640(3)	8.7867(8)	14.8409(10)	12.8913(8)
c/Å	13.0556(2)	17.6568(17)	22.412(2)	37.4502(14)
α/°	90	90	90	90
β/°	90	105.777(10)	110.351(10)	90.982(4)
γ/°	90	90	90	90
Volume/Å^3	2923.49(11)	1711.0(3)	5578.7(9)	7516.9(7)
Z	4	2	8	4
ρ_{calc}g/cm^3	1.383	1.678	1.311	1.253
μ/mm^{-1}	3.967	4.221	2.114	1.585
F(000)	1264.0	880.0	2304.0	2992.0
Crystal size/mm^3	0.15 x 0.15 x 0.1	0.3 × 0.2 × 0.2	0.5 × 0.4 × 0.15	0.49 × 0.19 × 0.15
Radiation	MoKα (λ = 0.71073)	MoKα (λ = 0.71073)	MoKα (λ = 0.71073)	MoKα (λ = 0.71073)
2θ range for data collection/°	6.74 to 50.69	6.966 to 52.74	6.674 to 50.7	6.52 to 50.7
Index ranges	-17≤h≤17, -18≤ k≤18, -15≤l≤15	-14≤h≤14, -10≤k≤10, -22≤l≤18	-21≤h≤20, -17≤k≤17, -13≤l≤26	-18≤h≤18, -15≤k≤12, -45≤l≤42
Reflections collected	38521	7617	10178	37268
Independent reflections	5363 [R_{int} = 0.0515, R_{sigma} = 0.0312]	3454 [R_{int} = 0.0464, R_{sigma} = 0.0722]	10178 [R_{sigma} = 0.1094]	13751 [R_{int} = 0.0677, R_{sigma} = 0.1093]
Data/restraints/parameters	5363/208/359	3454/0/219	10178/6/664	13751/350/982
Goodness-of-fit on F^2	1.047	1.027	1.119	1.045
Final R indexes [I>=2σ (I)]	R1 = 0.0532, wR2 = 0.1214	R_1 = 0.0413, wR_2 = 0.0861	R_1 = 0.0922, wR_2 = 0.2118	R_1 = 0.0786, wR_2 = 0.1714
Final R indexes [all data]	R1 = 0.0641, wR2 = 0.1278	R_1 = 0.0629, wR_2 = 0.0944	R_1 = 0.1318, wR_2 = 0.2279	R_1 = 0.1332, wR_2 = 0.1962
Largest diff peak/hole / e Å^{-3}	0.98/-0.88	1.11/-0.51	2.02/-1.62	1.76/-0.74

Table S2. Crystal data and structure refinement details for $\mathbf{2_{Dy}}$-$\mathbf{4_{Dy}}$.

Compound	$\mathbf{1_{Dy}}$	$\mathbf{2_{Dy}}$	$\mathbf{3_{Dy}}$	$\mathbf{4_{Dy}}$
Empirical Formula	$C_{32}H_{46}Dy_2$	$C_{44}H_{46}Dy_2Fe_2$	$C_{33}H_{37}DyN_2$	$C_{45}H_{51}DyN_2$
Formula Weight	755.69	1011.51	624.14	782.38
Temperature/K	150.03(10)	150	150	150
Crystal System	orthorhombic	Monoclinic	monoclinic	monoclinic
Space Group	$P2_12_12$	$P2_1/n$	$P2_1/c$	$P2_1/c$
a/Å	14.4524(9)	11.4410(5)	17.9045(7)	15.6469(6)
b/Å	15.4426(6)	8.8007(3)	14.8465(5)	12.9702(7)
c/Å	13.0677(5)	17.6498(7)	22.4149(10)	37.5845(12)
α/°	90	90	90	90
β/°	90	105.794(4)	110.370(4)	91.221(3)
γ/°	90	90	90	90
Volume/Å^3	2916.5(2)	1710.04(12)	5585.7(4)	7625.8(5)
Z	4	2	8	8
ρ_{calc}g/cm^3	1.721	1.964	1.484	1.363
μ/mm^{-1}	5.102	5.183	2.699	1.992
F(000)	1480.0	988.0	2520.0	3208.0
Crystal size/mm^3	0.1 × 0.1 × 0.08	0.838 × 0.751 × 0.42	1.094 × 1.048 × 0.729	0.761 × 0.326 × 0.287
Radiation	MoKα (λ = 0.71073)	MoKα (λ = 0.71073)	MoKα (λ = 0.71073)	MoKα (λ = 0.71073)
2θ range for data collection	6.442 to 52.78	7.142 to 52.788	6.958 to 52.798	6.496 to 50.696
Index ranges	-18≤h≤18, -19≤k≤19, -16≤l≤16	-14≤h≤14, -11≤k≤10, -18≤l≤21	-22≤h≤20, -18≤k≤18, -13≤l≤28	-18≤h≤17, -12≤k≤15, -45≤l≤45
Reflections collected	28480	10803	11385	49837
Independent reflections	5963 [R_{int} = 0.0702, R_{sigma} = 0.0775]	3477 [R_{int} = 0.0356, R_{sigma} = 0.0392]	11385 [R_{sigma} = 0.0582]	13634 [R_{int} = 0.0717, R_{sigma} = 0.0855]
Data/restraints/parameters	5963/260/359	3477/0/219	11385/0/664	13634/662/983
Goodness-of-fit on F^2	1.084	1.096	1.135	1.212
Final R indexes [I>=2σ (I)]	R_1 = 0.0728, wR_2 = 0.1626	R_1 = 0.0285, wR_2 = 0.0629	R_1 = 0.0718, wR_2 = 0.1571	R_1 = 0.0893, wR_2 = 0.1593
Final R indexes [all data]	R_1 = 0.0898, wR_2 = 0.1727	R_1 = 0.0315, wR_2 = 0.0642	R_1 = 0.0842, wR_2 = 0.1632	R_1 = 0.1168, wR_2 = 0.1705
Largest diff peak/hole / e Å^{-3}	3.52/-2.08	1.94/-1.48	4.34/-1.97	2.48/-1.76

Magnetic property measurements. The magnetic properties of $\mathbf{1_{Dy}}$-$\mathbf{4_{Dy}}$ were measured on a Quantum Design MPMS-7 SQUID magnetometer in a temperature range of 1.8-300 K. The SQUID samples were prepared in the glove-box by restraining a crystalline sample in eicosane, contained in an NMR tube sealed with a J. Youngs valve. The samples were then placed under vacuum and flame-sealed.

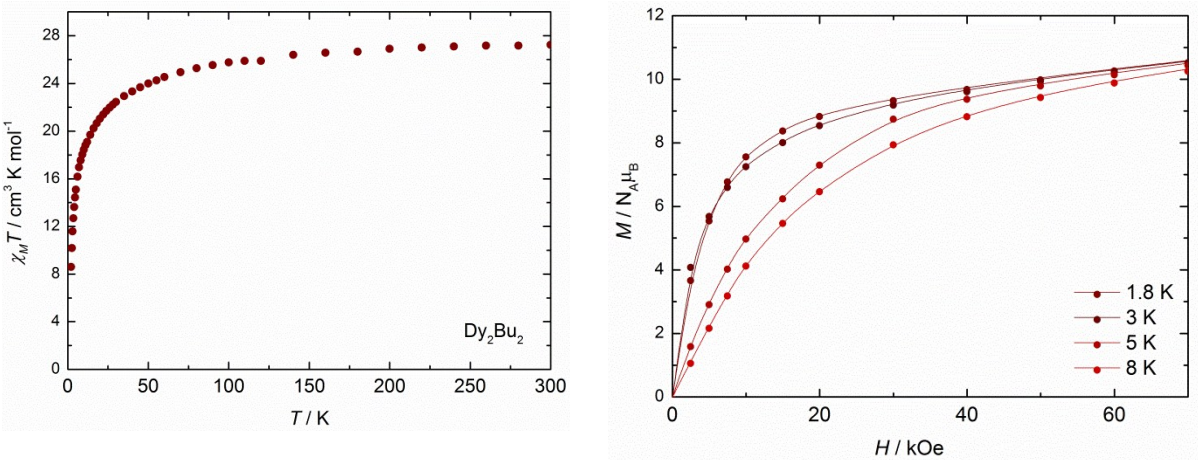

Figure S21. Left: temperature dependence of $\chi_M T$ for $\mathbf{1_{Dy}}$ in an applied field of 1000 Oe. Right: field dependence of the magnetisation for $\mathbf{1_{Dy}}$ at 1.8-8 K. Solid lines are a guide for the eye.

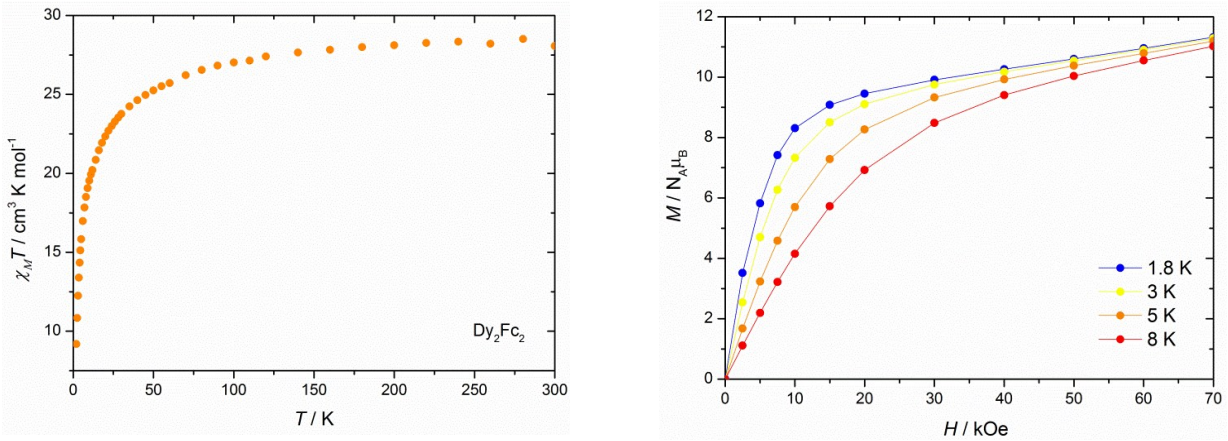

Figure S22. Left: temperature dependence of $\chi_M T$ for $\mathbf{2_{Dy}}$ in an applied field of 1000 Oe. Right: field dependence of the magnetisation for $\mathbf{2_{Dy}}$ at 1.8-8 K. Solid lines are a guide for the eye.

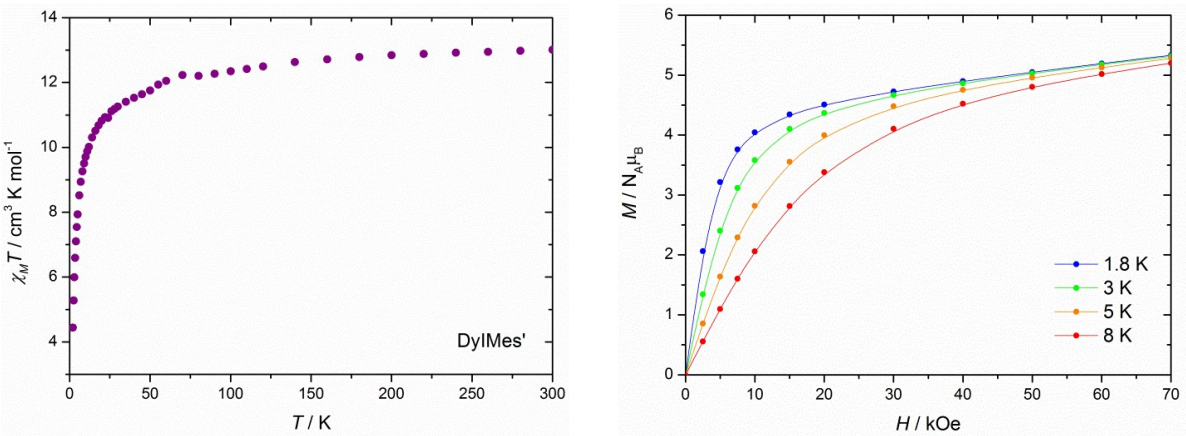

Figure S23. Left: temperature dependence of $\chi_M T$ for $\mathbf{3_{Dy}}$ in an applied field of 1000 Oe. Right: field dependence of the magnetisation for $\mathbf{3_{Dy}}$ at 1.8-8 K. Solid lines are a guide for the eye.

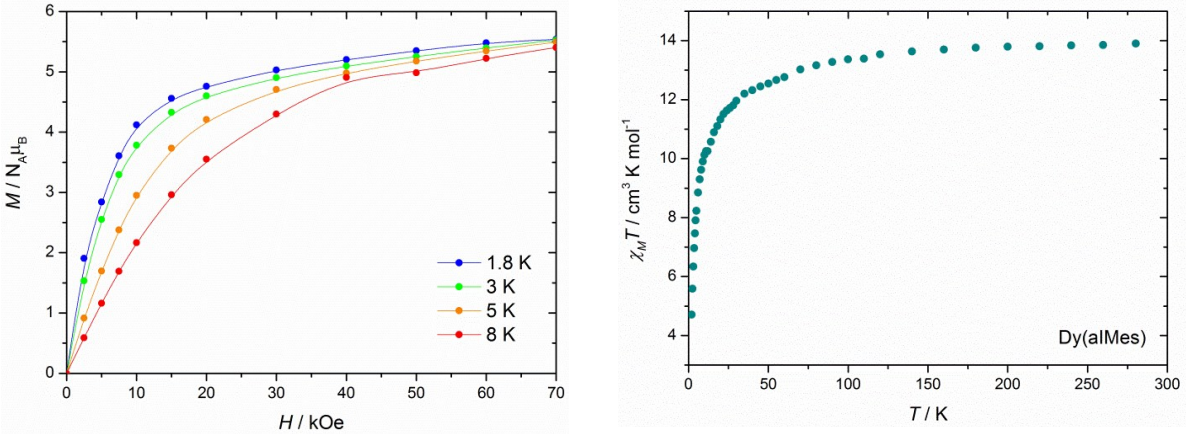

Figure S24. a) Field dependence of the magnetisation for $\mathbf{4_{Dy}}$ at 1.8-8 K – solid lines are a guide for the eye; b) the product of molar magnetic susceptibility and temperature against temperature for $\mathbf{4_{Dy}}$.

---

[1] G. Wilkinson and J. M. Birmingham, *J. Am. Chem. Soc.*, 1954, **76**, 6210.

[2] X. Bantreil and S. P. Nolan, *Nat. Protocols*, 2011, **6**, 69-77

[3] A.L.Spek, *Acta Cryst.*, 2009, **D65**, 148-155.

[4] O.V. Dolomanov, L. J. Bourhis, R. J. Gildea, J. A. K. Howard, H. Puschmann, J. Appl. Cryst., 2009, **42**, 339

[5] G. M. Sheldrick, Acta Cryst., 2015, **A71**, 3

[6] G. M. Sheldrick, Acta Cryst., 2015, **C71**, 3